Front. Earth Sci. 2018, 12(2): 349–360
https://doi.org/10.1007/s11707-017-0655-y

RESEARCH ARTICLE

Spatial and temporal correlation between beach and wave processes: implications for bar–berm sediment transition

V. JOEVIVEK (✉)[1,2], N. CHANDRASEKAR[1], S. SARAVANAN[1], H. ANANDAKUMAR[2], K. THANUSHKODI[2], N. SUGUNA[2], J. JAYA[2]

1 Centre for GeoTechnology, Manonmaniam Sundaranar University, Abishekapatti, Tirunelveli 627012, Tamil Nadu, India
2 Akshaya college of Engineering and Technology, Kinathukadavu, Coimbatore 642109, Tamil Nadu, India

© Higher Education Press and Springer-Verlag Berlin Heidelberg 2017

Abstract Investigation of a beach and its wave conditions is highly requisite for understanding the physical processes in a coast. This study composes spatial and temporal correlation between beach and nearshore processes along the extensive sandy beach of Nagapattinam coast, southeast peninsular India. The data collection includes beach profile, wave data, and intertidal sediment samples for 2 years from January 2011 to January 2013. The field data revealed significant variability in beach and wave morphology during the northeast (NE) and southwest (SW) monsoon. However, the beach has been stabilized by the reworking of sediment distribution during the calm period. The changes in grain sorting and longshore sediment transport serve as a clear evidence of the sediment migration that persevered between foreshore and nearshore regions. The Empirical Orthogonal Function (EOF) analysis and Canonical Correlation Analysis (CCA) were utilized to investigate the spatial and temporal linkages between beach and nearshore criterions. The outcome of the multivariate analysis unveiled that the seasonal variations in the wave climate tends to influence the bar – berm sediment transition that is discerned in the coast.

Keywords beach, nearshore, sandbar, grain size, empirical orthogonal function, canonical correlation analysis

1 Introduction

The coastal region from the sea to the land can be divided into five categories: offshore, nearshore, foreshore, backshore, and dune. Among these, the nearshore and the foreshore are comparatively sensitive over a short period of time owing to the interaction between the beach and the incoming waves (Short, 2012). The nearshore is the zone in which the wave action yields breaking waves, longshore current, and littoral transport; in contrast to this the foreshore zone lies between the mean low tide and the seaward beach berm which controls the morphodynamic state of the beach system. The seasonal trends have influenced a fair trade-off between the beach and the swash zone by means of cross-shore sediment transport. Such transition yields the cyclic process of two coastal environments: one is a flat berm with multiple sandbars in the surf zone and the other is a developed berm but absence of sandbars in the surf zone. This consequently proved that a possible correlation exists between the wave climate and the beach morphology (Joevivek and Chandrasekar, 2014). The diverse studies confirm this statement by various modes of beach and wave dynamics studies.

Bascom (1953) carried out a study on temporal correlation between the foreshore slope and sandbar formation along Carmel beach, California. His finding insinuates that the beaches attained flat foreshore with multiple nearshore bars during the high energy wave condition whereas steep foreshore with zero to one nearshore bar during low energy wave condition. Correspondingly, Wright and Short (1984) categorized the beach system as a reflective, intermediate, and dissipative state based on the monsoonal wave climate, while, in contrast to that, Galvin (1968) proposed a semi-empirical formula for evaluating the breaking wave type in the nearshore environment. Fascinatingly, the results of the beach morphodynamic state and breaking wave type with respect to the seasonal variations were consistent with the findings of Bascom (1951, 1953, 1964).

Many studies have been focused on the spatial and temporal relationship between the beach and the nearshore environment (e.g., Hunter et al., 1979; Araya-Vergara, 1986; Xie and Liu, 1987; Wang et al., 1998; Miller, 1999;

Received October 3, 2016; accepted March 15, 2017

E-mail: vjoevivek@gmail.com

Miselis and McNinch, 2006; Maanen et al., 2008; Saravanan et al., 2013; Joevivek and Chandrasekar, 2014; Splinter et al., 2014). The outline of these studies suggested that the wind and wave current are the dominant forces controlling the beach and nearshore morphology. The evaluation of numerical techniques in the past four decades has led to meticulous solutions for modeling nearshore dynamics with different wave conditions. Empirical orthogonal function (EOF) analysis is an extensively used method for identifying spatial and temporal correlation of beach and nearshore morphology (Winant et al., 1975; Shenoi et al., 1987; Nayak and Chavadi, 1988). Both the theory and mathematical representation of EOF analysis is prescribed in detail by Svensson (1999). Recently, Harley et al. (2015) applied EOF technique to express the cross-shore processes in an embayed beach system. The result of correlations between the beach, nearshore, and offshore wave parameters contributed magnitude and direction of suspended sediment transport is relative to the breaking point. The canonical correlation analysis (CCA) is a similar technique which can provide a temporal correlation of the beach and wave parameters. Diverse studies have proven its effectiveness in the realm of coastal engineering (e.g., Clark, 1975; Larson et al., 2003; Różyński, 2003; Hardoon et al., 2004; Horrillo-Caraballo and Reeve, 2011). Różyński (2003) used both EOF and CCA techniques to investigate multiple longshore bars and their interactions. The combined analysis of EOF and CCA outcomes provides a detailed physical explanation of interaction between shoreline and sandbars.

Several numerical models have been introduced to enhance understanding of complex coastal systems (Masselink et al., 2008; Ruessink et al., 2009; Pape et al., 2010a, b; Blossier et al., 2016). For example, Hsu et al. (2006) introduced a wave-resolving boundary layer model for predicting the onshore migration of a sandbar. The model combines wave-driven morphological parameters to govern the bottom stress and near-bed sediment transport. This model efficiently predicted dominant mechanisms of sediment transport and is consistent with previously developed wave models. Similarly, Marino-Tapia et al. (2007a, b) investigated cross-shore sediment transport on natural beaches and its relation with sandbar migration patterns. They proffered field-based parameterization (shape function) to evaluate the mechanism of cross-shore sediment transport with respect to the hydrodynamic and beach morphological conditions. The shape function consistently explained the nearshore sandbar migration. Broekema et al. (2016) deployed Delft 3D model to examine the cross-shore morphodynamics and sediment sorting processes for a barred beach. This model explicates the infragravity (IG) wave effects on cross-shore beach profile and clearly shows the sediment sorting processes beneath the high and the moderate wave conditions. Though these reports delineate the physical process of wave and beach morphology, there is still a slot that is left for the exploration of constructive and destructive linkage between the beach and wave parameters during the bar-berm sediment transition. This paper proceeds towards this concern through field examination and multi-criteria decision analysis.

2 Study site

The dataset used in the present study was collected at Nagapattinam beach, central Tamil Nadu coast, India (Fig. 1). The sand present in the beach with a noticeable reddish/black color proves the enrichment of economic placer deposits present in the coast (Joevivek and Chandrasekar, 2014). The relief on the north and south of the Nagapattinam coast is interfered by estuaries, lagoons, and creeks. The coast experiences three seasons in a year, namely, southwest (SW) monsoon, northeast (NE) monsoon, and fair weather periods. During the study period, predominant wind directions are found through the northeast, southwest, southeast and south. The beach encountered both the high and low tide twice in a day which delineates semidiurnal tide condition observed in the coast. The reference tidal chart manifests that the mean high tide range is about 0.68 m and the mean low tide range is about 0.28 m (Chart No. 3007, scale 1:35,000, year 2010, published by NHO, Dehradun). Wind speed is normally from 11 to 26 km/h over an annual cycle. However, it exceeds 75 km/h during the NE monsoon owing to the tropical cyclones.

3 Data and methods

In this paper, methodology part includes two sub-sections: the first section reports a comprehensive set of observations of beach and nearshore parameters. The second section illustrates the spatial and temporal analysis of beach and wave dynamics with the aid of empirical models.

3.1 Field data

The cross-shore beach profile was achieved on a monthly and seasonal basis from January 2011 to January 2013 at a spring low-tide period. A Trimble M3 total station was deployed to measure the monthly and seasonal beach profile which is capable of measuring distance with an accuracy of < 3 mm in normal weather conditions. The accuracy of vertical (angle) measurement is 1.5 mgon (0.00135°) based on the DIN 18723 standard system. During this survey, the total station was set up over a known bench mark using tripod accessories. The accuracy locations of benchmark and tail point are fixed by the real-time kinematic global positioning systems (RTK-GPS) in

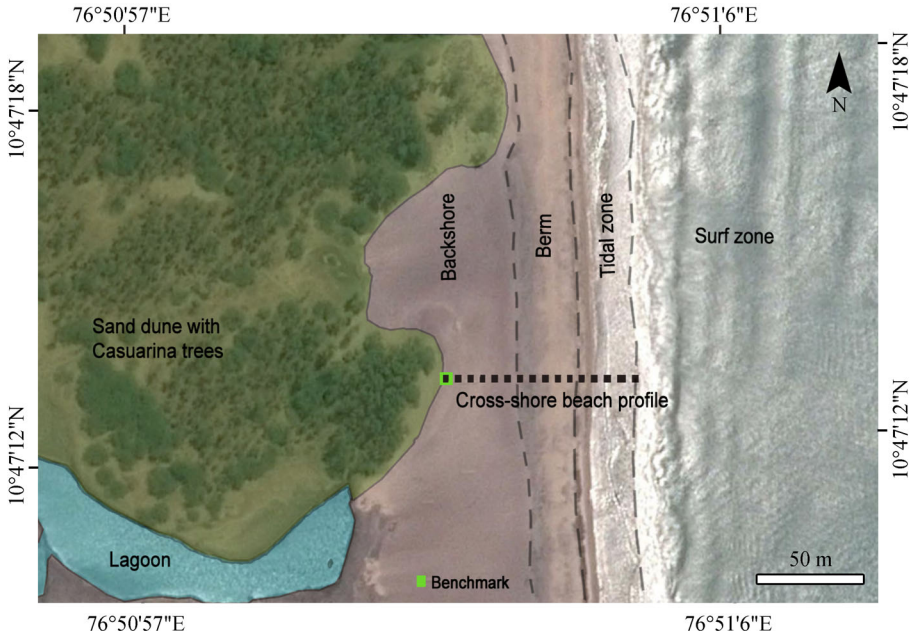

Fig. 1 Location map of the study area. The dotted line shows cross-shore profile segment and green block is the fixed benchmark.

order to achieve a perfect cross-shore profile. A flat footer was attached at the bottom of the prism rod in order to avoid the penetration of rod into the beach sand. The cross-shore variations were recorded along the profile transect for every 2 meters. At each point, distance and angle with respect to the benchmark were recorded in the total station unit and elevation was calculated automatically by the internal processor. The measured data were refined by subtraction of instrumental errors. The OceaN WavE Tool (ONWET) standalone software package (Joevivek and Chandrasekar, 2016) was utilized to evaluate beach width (actual distance between benchmark and low tide region), foreshore slope, and beach sediment volume (volume of sediment accumulated between benchmark and low tide region).

Breaking wave height (Hb) of the Nagapattinam beach is measured by calibrated levelling with millimeter (mm) scale accuracy. The levelling staff is fixed at the low-tide region and the height of the breaking waves is measured from the line of sight to the wave crest and horizon (Bascom, 1964). Significant wave height is attained at the one third of the successive breaking waves. Likewise, the total station is used to measure the surf zone width by calculating distance between the boat at the breaker zone and the low tide region. Wave period (T) is measured by the digital stop clock. The predominant wave period (T) is computed from the average time period of 300 successive waves. The longshore current velocity is measured by the buoyant plate floating a distance 2 minutes beyond the breaker point (Jayakumar et al., 2004). The wind and tide data were utilized from the online resource (https://www.windfinder.com/).

Sediment samples were collected at the inter-tidal zone by using an aluminium grabber with a single open edge. The samples were packed and properly labelled for laboratory analysis. About 100 grams of samples were extracted by the coning and quartering method. After being soaked in water, the samples were perturbed by a mechanical stirrer to disaggregate them and to withdraw the clay fractions. The samples are further processed by H_2O_2 and dil. HCL for separation of organic contents, inorganic contents, and fine broken shells. The treated samples were sieved in a Ro-Top machine with quarter phi interval mesh grids ranging from $+40$ to $+230$ ASTM units. The textural characteristics of these sieve fractions were extracted by using the method of moments (Folk and Ward, 1957; Blott and Pye, 2001).

3.2 Statistical analysis

3.2.1 Empirical Orthogonal Function (EOF) analysis

The Empirical Orthogonal Function (EOF) provides spatial and temporal variation in a beach profile dataset using the principal eigenfunctions. In this study, the ONWET standalone software is deployed to estimate spatial and temporal eigenfunctions of the profile data set. The result of first eigenfunction grasps the greatest portion of the mean square value. The second and third eigenfunction comprises the residual part. The first spatial eigenfunction (U1) holds mean beach profile of the original data. The second (U2) and third (U3) eigenfunctions stands for the bar-berm sediment transition and the sediment sorting respectively. Similarly, first temporal eigenfunction (V1)

spots out a comprehensive accretion / erosion in the profile transect over the study period. The second (V2) and the third (V3) eigenfunctions stipulates temporal variation in sediment transport and grain size distribution.

3.2.2 Canonical Correlation Analysis (CCA)

The canonical correlation analysis (CCA) provides a linear correlation between the two multi-dimensional datasets. CCA correlations of nearshore (Y1) and the beach morphology (Y2) were extracted from XLSTAT 4.0 add-on statistical tool in Microsoft Excel environment (available online at https://www.xlstat.com/). The nearshore variables: wave period (T), breaking wave height (Hb), longshore current velocity (V), and surf zone width (W) were considered as one phase (Y1) whereas beach morphological variables: beach width, nearshore slope, and sediment volume were considered as another phase (Y2). Canonical variables (or canonical function coefficients) were formulated by the regression coefficients of the input variables (i.e., Y1 and Y2). The results of F1, F2, and F3 factors dispensed variability in the dataset which helped to figure out the correlations between canonical variables and input variables. Tri-plot is contrived for F1 and F2 factors to analyze the spatial and the temporal correlation between the beach and the wave dynamics. The upshot from the graphical chart is interpreted by the projection of lines. The length and the position of the lines denote the intensity of the positive or negative correlation of Y1 and Y2 variables.

4 Results and discussion

4.1 Wave mechanism

The wind and wave currents are the significant parameters that predominate the littoral transport in the present study area (Sanil Kumar et al., 2002). The waves generated the turbulence force that prompts necessary energy for sediment transition between beach and nearshore zone. The shape and size of the nearshore deposits, in turn, gave rise to the changes in the uprush / backwash wave energy with respect to changes that occurred in the nature of wave breaking. The spatial and the temporal variability of the wind and the wave parameters are shown in Table 1. According to field observation, the wind approaches the coast from the NE during the northeast monsoon, SW and S during the southwest monsoon, and SE and S during the fair weather period. During the NE monsoon, the wind and waves are unidirectional so that waves approaching the coast will be energetic during this period. The energetic waves have eroded the berm and the intertidal sediments and carried it towards offshore, but most of it was deposited at the surf zone due to the collision between the uprush and the backwash waves. This continuous phenomenon creates numerous sandbars in the surf zone. During the SW monsoon, offshore wind and wave energy is slackened-off by the onshore wind force. Hence, the offshore sediment transport is more feeble than the onshore sediment transport. The average wind speed rises up to 26 km/h during the SW monsoon. During this period, the longshore current is configured in such a way that it is parallel to the shore in the direction of exclusion of the wind. Therefore, onshore sediment transport produces well developed berm at the foreshore region. The tide data provided in Table 1 exhibits microtidal condition over an annual cycle. The rise and fall of the tidal level will influence the sediment discharge with respect to the monsoonal wind and wave conditions.

The wave period has varied scaling from 7 to 12 seconds over an annual cycle. The wavelength was observed to be shorter in the NE monsoon and larger in the SW monsoon which conveys that the SW monsoon executed surging waves while the NE monsoon executed spilling waves. Both the monthly and seasonal variation of breaking wave height (Hb) unveils that the wave height is high during the NE monsoon, but less during the SW monsoon and moderate in fair weather conditions. Similarly, the longshore current velocity (V) reveals that the waves attained maximum velocity during the NE monsoon and the minimum during the rest of the study period. This implies that the waves during NE monsoon are likely to erode the sediments from the berm and tidal region and carry it to the nearshore resulting in the formation of numerous sandbars that develop in the surf zone region (Figs. 2(a) and 2(d)). During the extended periods of non-monsoonal conditions, the sandbars tend to slowly sweep off shore due to the wave energy and likely get deposited in the tidal and the berm region (Figs. 2(b) and 2(c)). The results of the surf zone width authenticate this statement, because a broader surf zone with multiple sandbars can be observed during the NE monsoon. Whereas the short surf zone width yielded during the SW and the non-monsoon suggest the absence of sandbars or perhaps one sandbar present in the nearshore.

4.2 Beach morphology

The field data collected from the month of January 2011 till the month of January 2013 (on a monthly and seasonal basis) could yield an extensive dataset to resolve the temporal changes of the beach morphology (Fig. 3). During the NE monsoon, the variation in the berm and the foreshore slope indicates that the undertow erodes sand materials from the berm and the tidal region and carries it towards the sea. During the SW and the non-monsoon seasons, the surging wave transports the suspended sediments from the nearshore to the foreshore region and does not retrieve it because of the associated backwash. As

Table 1 Wind and wave data of Nagapattinam coast during the study period

Period	Dominant wind direction	Average wind speed/(km·h^{-1})	Mean tide level/m (High tide/low tide)	Wave period /s	Breaker wave height/m	Longhsore current velocity /(m·s^{-1})	Surf zone width/m
Jan-11	NE (45°)	22	0.6 / 0.22	8	0.98	0.5	46
Feb-11	NE (45°)	19	0.55 / 0.23	9	0.81	0.08	55
Mar-11	SE (135°)	17	0.61 / 0.25	9	0.78	0.13	46
Apr-11	SE (135°)	14	0.62 / 0.24	10	0.86	0.24	44
May-11	S (180°)	25	0.73 / 0.22	10	0.76	0.24	32
Jun-11	SW (225°)	23	0.66 / 0.22	9	0.54	0.17	29
Jul-11	SW (225°)	26	0.67 / 0.23	11	0.59	0.11	24
Aug-11	SW (225°)	23	0.64 / 0.21	10	0.63	0.11	27
Sep-11	S (180°)	19	0.73 / 0.29	12	0.53	0.13	21
Oct-11	S (180°)	12	0.68 / 0.24	11	0.61	0.19	46
Nov-11	NE (45°)	21	0.65 / 0.23	9	0.91	0.25	52
Dec-11	NE (45°)	23	0.71 / 0.25	8	1.18	0.43	47
Jan-12	NE (45°)	24	0.66 / 0.24	7	1.03	0.43	41
Apr-12	SE (135°)	13	0.61 / 0.22	10	0.75	0.22	32
Jul-12	SW (225°)	24	0.69 / 0.23	10	0.52	0.15	25
Oct-12	S (180°)	11	0.67 / 0.25	11	0.41	0.09	17
Jan-13	NE (45°)	21	0.69 / 0.22	8	0.98	0.32	48

observed in the beach morphological parameters in Table 2, from the month of January till April, the width of the beach gradually increases and is found to be high during the SW monsoon. The onshore drive of the seawater along with the suspended sediments creates an accumulation of sediments in the beach and the width of the beach increases considerably and provides the maximum deposition in these zones. However, seasonal changes from SW to NE produce a decreasing trend of beach width. This is due to the high wave energy and reversal trend in the direction of sediment transport that occurs during the NE monsoon. The slope of the beach is the angle formed by the intersection between the plane of the beach and the horizontal plane of the sea-water surface. The beach attained the maximum steep slope during the SW monsoon and gentle slope during northeast monsoon and fair weather periods. This cyclic condition conveys that the beach attained an equilibrium condition through the foreshore-nearshore sediment transport (Reis and Gama, 2010). The volume of the sediment observed in the beach undergoes typical seasonal changes due to the hydrological conditions and longshore sediment transport. In Table 2, volumetric data disclosed that the beach exhibits high volume of sediments during the SW and non-monsoon condition while the less volume of sediments during the NE monsoon. This proves a process of seasonal wave action taking place which shifts the sand materials from the berm to the bar and vice-versa (Bascom, 1951).

4.3 Bar – berm sediment transition

4.3.1 Grain size distribution

Grain size analysis has been performed to understand the depositional environment of the beach sediments that is found in the coast. The size and texture of the grains at the tidal region not only establish the influence of sediment sources, but also the influence of hydrodynamics of the coast (Hunter et al., 1979; Liu and Zarillo, 1989). The weight percentage of sediment distribution in Fig. 4 shows the mixing of the sediment populations which includes one predominant and one subordinate population that exhibits bimodal distribution perceived in the coast. The maximum population of bimodal distribution peaked at 1.75–2.25 phi showed that the deposition of medium to fine sand can be observed throughout the study period (Blott and Pye, 2001).

The mean and the sorting of the tidal samples show that the medium sand can be perceived during the SW and non-monsoon conditions, while the fine sand can be perceived during the NE monsoon (see Table 2). It implies that waves during the SW monsoon have less energy flux compared to the NE monsoon. The less turbulence force of backwash could not take away sediments from the foreshore to the nearshore and therefore well-sorted medium grains were deposited in the berm region. During this period, the winnowing action by open sea remains the cause of the

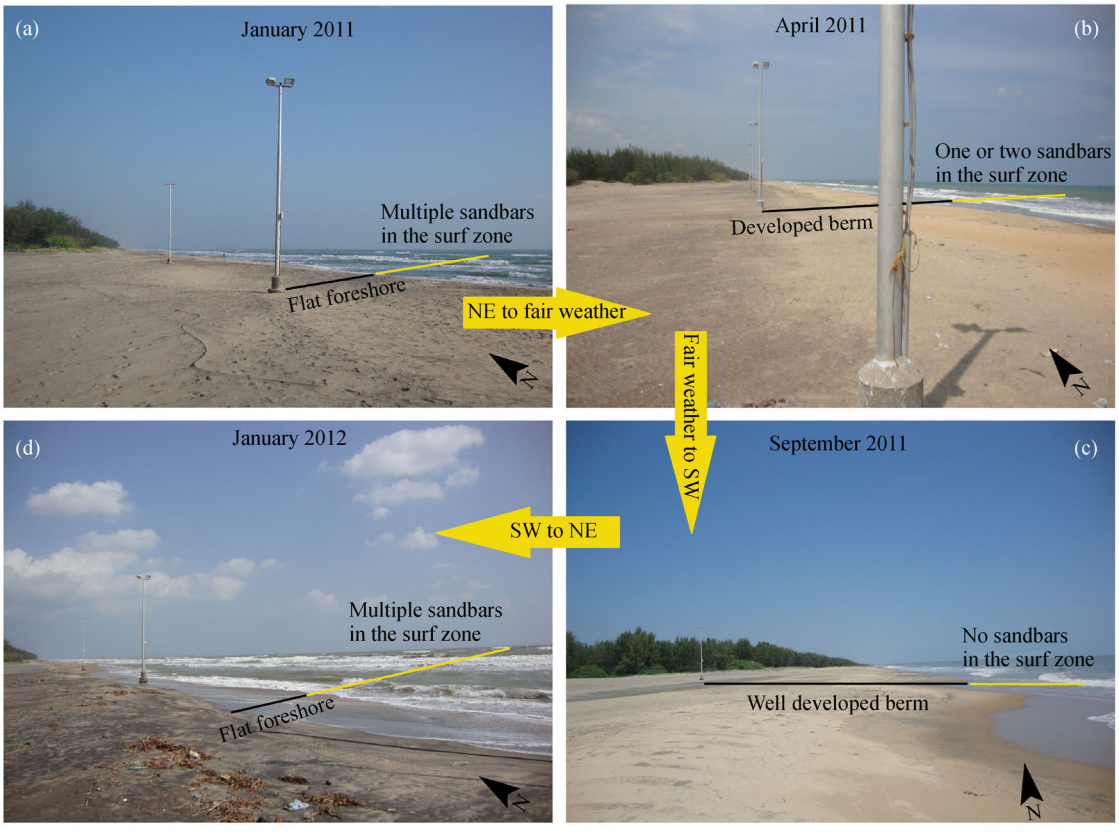

Fig. 2 Seasonal variation of bar-berm sediment transition. (a) Flat berm with numerous sandbars (January 2011), (b) developing berm surface with few sandbars (April 2011), (c) well developed berm with absence of sandbars (October 2011), (d) short berm with numerous sandbars (January 2012). It is interesting to note that beach condition in January 2012 is almost similar to the January 2011. The arrow in yellow color demarcates seasonal variation over an annual cycle.

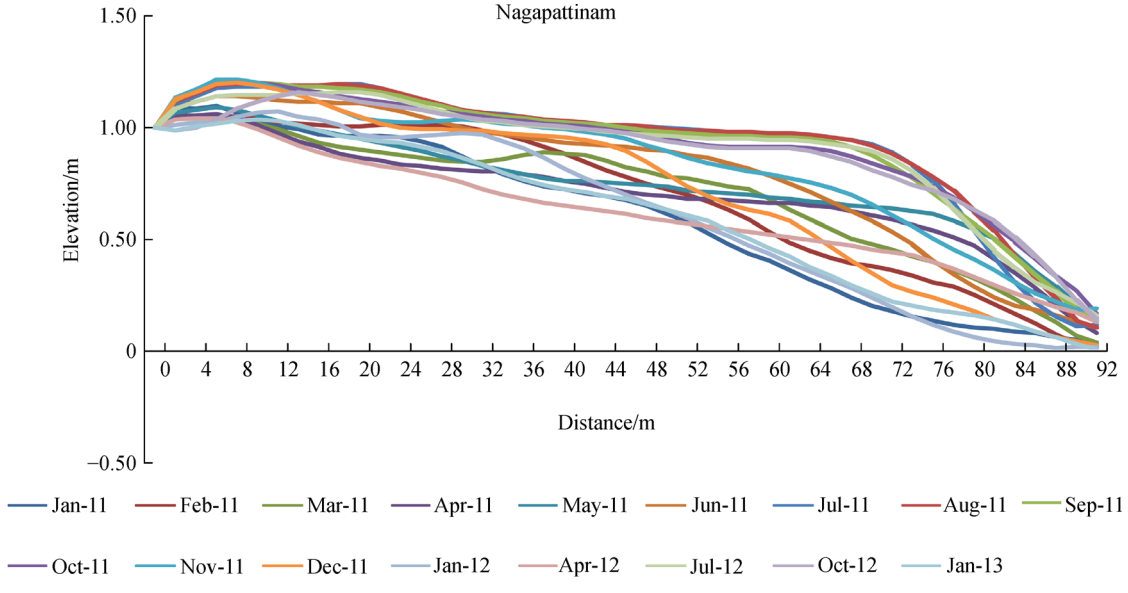

Fig. 3 Cross-shore beach profile during the period between January 2011 and January 2013.

Table 2 Beach morphology and texture of foreshore sediments

Period	Beach morphology			Grain size characteristics (Method of moment)	
	Beach width	Foreshore slope	Beach sediment volume	Mean/phi	Sorting/phi
Jan-11	76	2.6	47.06	2.15	0.74
Feb-11	81	3.8	52.34	2.04	0.76
Mar-11	84	3.14	55.18	2.05	0.75
Apr-11	83	3.24	57.08	2.01	0.75
May-11	84	5.11	61.96	1.96	0.74
Jun-11	86	7.06	66.61	1.92	0.73
Jul-11	88	6.45	76.84	1.88	0.73
Aug-11	89	9.08	78.65	1.86	0.73
Sep-11	92	10.79	76.83	1.88	0.72
Oct-11	87	7.59	74.06	2.06	0.72
Nov-11	83	3.44	69.35	2.21	0.72
Dec-11	80	1.7	60.44	2.47	0.68
Jan-12	67	1.2	28.29	2.44	0.69
Apr-12	78	4.74	36.87	2.08	0.73
Jul-12	86	7.25	76	1.93	0.71
Oct-12	88	8.59	74.37	2.06	0.74
Jan-13	79	1.9	43.55	2.13	0.75

accumulation of fine sediments at the backshore region. The strong turbulence force of uprush and backwash tends to transport the sediments from the foreshore to the nearshore and offshore region. The rest of the well sorted fine grains settled as thick laminated sand patches at the intertidal zone. Hence, coast experienced the predominance of fine sand during the NE monsoon.

4.3.2 Empirical Orthogonal Function (EOF) analysis

The first three spatial and temporal eigenfunctions represent more than 99.792% of the total variability of the cross-shore beach profile data (Table 2). The first spatial eigenfunction (U1) of the monthly and the seasonal data indicates that the surface of the beach is a gentle slope up to 55 m from the reference point (Fig. 5). It implies that the landward wind energy controls the backshore morphology. The variation of the slope from the berm to the tidal region revealed the possibility of sand bar formation in the nearshore zone. The first temporal eigenfunction (V1) yields the cyclic pattern which denotes the nearly equilibrium condition observed in the coast. The variation

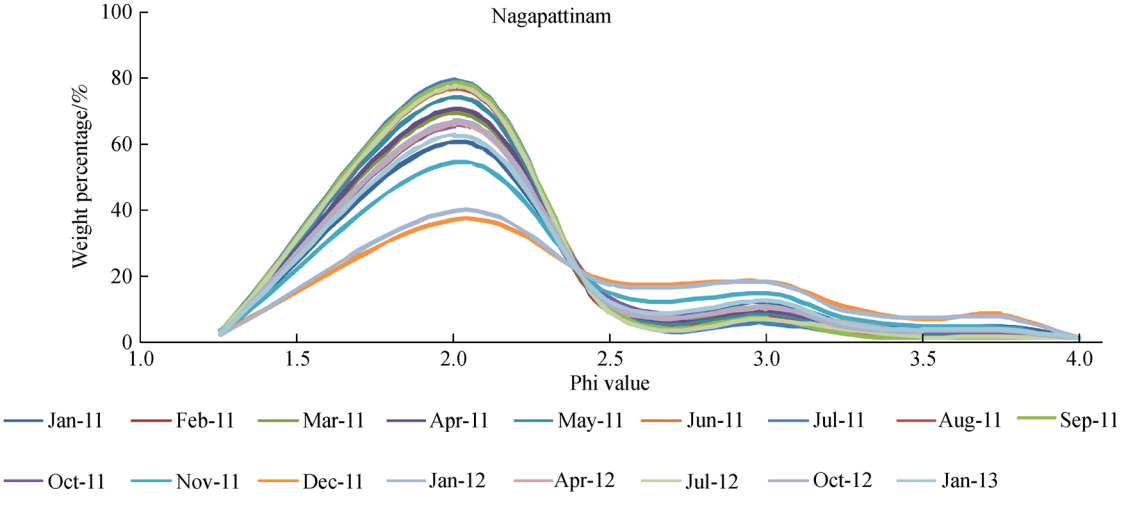

Fig. 4 Grain size distribution at the foreshore region.

in the eigenfunction from crest to trough establishes the changes taking place in a monsoonal climate from the NE to SW and vice-versa. The second spatial eigenfunction (U2) shows the bar-berm sediment transition between the tide, berm, and backshore region. It reveals that the wave process have influenced sediment transition between backshore and dune region. The second temporal eigenfunction (V2) designates the overall deposition of the beach that is achieved through two conspicuous cycles of erosion and deposition. It implies that the maximum deposition occurred during the SW monsoon and maximum erosion during the NE monsoon. The third spatial eigenfunction (U3) describes the sorting nature of the grain size distribution. The grain size distribution is symbolically denoted by 'V' or 'inverted 'V' shape of the third eigenfunction. The 'V' shaped nature of U3 at the berm area shows the well sorted sediments while inverted 'V' shape at backshore and tidal region illustrates the moderately sorted sediments (Joevivek and Chandrasekar, 2016). The size distribution of grains in Table 1 validates this statement. The third eigenfunction (V3) denotes the size of the grains varied with respect to the seasonal changes. The higher the variation in the grain size distribution from the month of November to December proves that the dynamic wave climate was caused by the tropical cyclones.

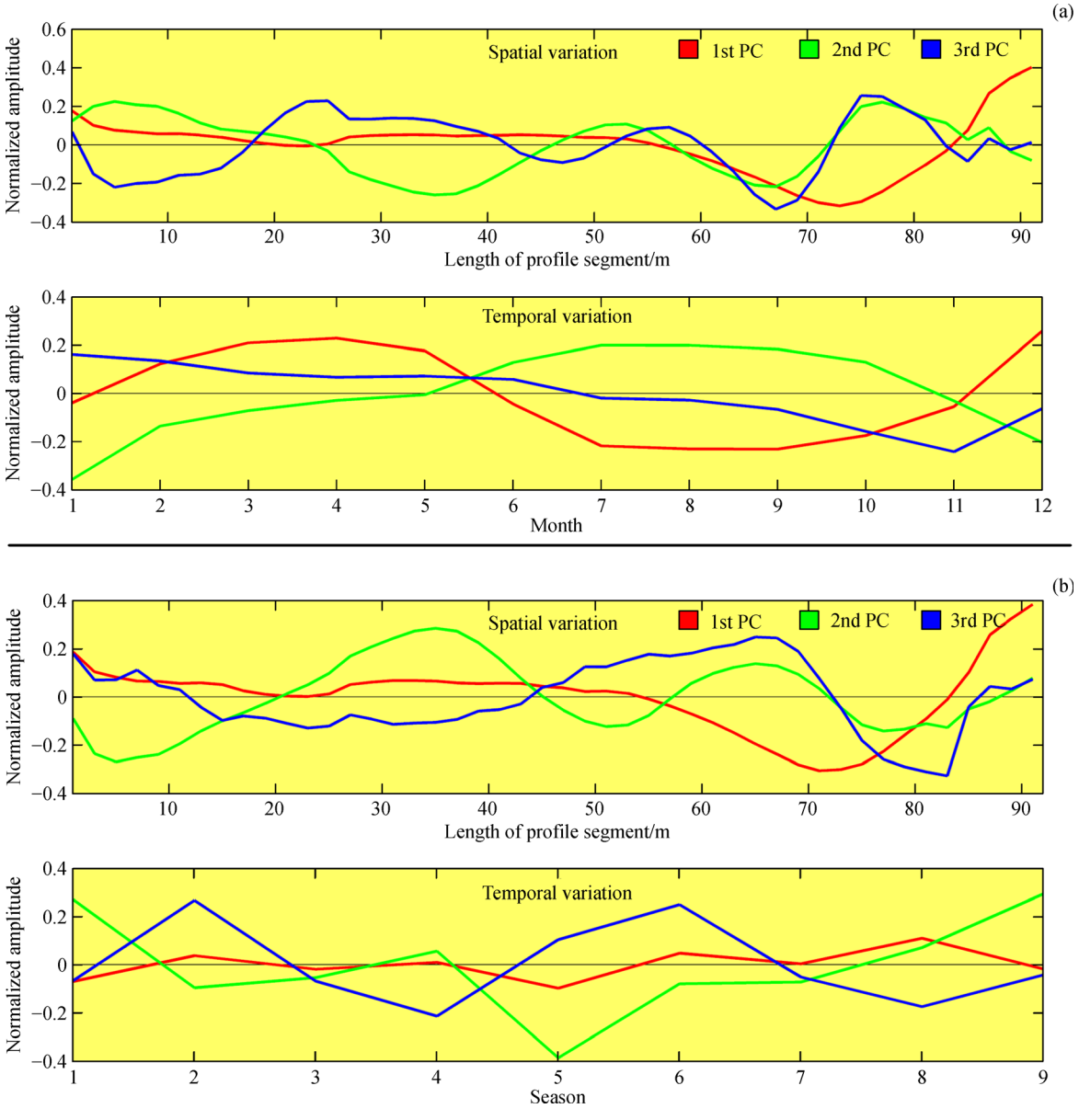

Fig. 5 EOF results show spatial and temporal variation of the beach morphology. (a) Monthly variation (January 2011 to December 2011), (b) seasonal variation (January 2011 to January 2013).

4.3.3 Canonical Correlation Analysis (CCA)

The correlation between nearshore variables and beach morphology on a monthly basis are derived from CCA analysis. The eigenvalues, variability, and cumulative percentage in Table 3 represent the strength of the axes (or factor) with respect to the nearshore variables (Y1) and beach morphology (Y2). Factor 1 along with factor 2 includes 90.651% of the total variance. The lines observed from the graph represent the degree of correlation between two variables (Fig. 6). From the results of CCA triplot, the breaking wave height, longshore current velocity, and surf zone width manifest a positive correlation. Concurrently, it is noted that the wave period anti-correlated with the surf zone width. This conveys that the wave period is less when the surf zone width is high. It is because the wider surf zone precisely expresses the presence of multiple sandbars at the nearshore region. Hence, wave period shortens as a result of sandbars breaking the incoming waves. As compared to the nearshore variables, beach morphological parameters, namely, the beach width, foreshore slope, and sediment volume are negatively correlated in the CCA plot. Beach sediment volume is anti-correlated with breaking wave height and this highlights the sediment transition between the beach and nearshore. Higher breakers possess high wave energy which has the capability of eroding sediments from the berm and tidal region. The eroded sediments have been placed by the subsequent waves, hence presence of a series of sandbars can be observed in the nearshore region. During this process, the beach sediment volume is considerably reduced. Similarly, foreshore slope is anti-correlated with longshore current velocity. The low current velocity provides less turbulence force so that sediments are deposited at the foreshore region. Repetition of this process creates steep sloping nature. Finally, it is understood that the wave process dominates the beach morphology by bar – berm sediment transition.

4.3.4 Sediment transport rate

The longshore sediment transport rate (Q) provides a clear understanding of bar–berm sediment transition. Here, the outcome of sediment transport rate is used for validating EOF and CCA results. A simple mathematical formula proposed by Walton and Bruno (1989) is deployed to

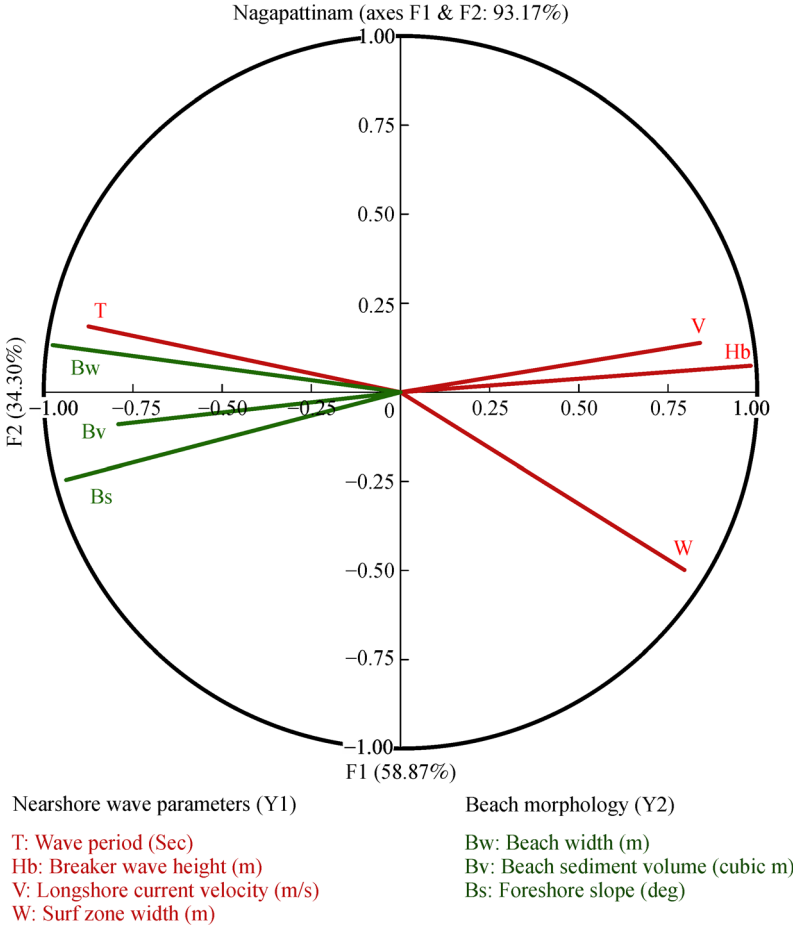

Fig. 6 CCA results showing correlation between beach and wave dynamics. The red color indicates nearshore parameters and green color indicates beach morphological parameters.

Table 3 Percentage of variance obtained from EOF and CCA analysis

EOF analysis	First eigenfunction (λ1)	Second eigenfunction (λ2)	Third eigenfunction (λ3)
Variance (%)	92.1349	7.4909	0.1662
Cumulative (%)	92.1349	99.6258	99.792
CCA analysis	**Factor (F1)**	**Factor (F2)**	**Factor (F3)**
Eigenvalue	0.840	0.443	0.132
Variability (%)	59.329	31.322	9.349
Cumulative (%)	59.329	90.651	100.000

estimate the longshore sediment transport between January 2011 and December 2011. According to the seasonal variations, a change in the direction of longshore sediment transport can be observed in the graphical plot (Fig. 7). During the NE monsoon, sediments are transported southward. The convergence of waves will enhance the wave energy so that backwash migrates the beach sediments towards the sea. However, migrated sediments get settled at the nearshore due to the collision between the uprush and the backwash waves. This process continues leading to the formation of sandbars at the surf zone. The results between the March and September attested the less sediment transport, which ultimately expose maximum accretion of sediments in the foreshore region. The divergence of the wave process dissipates the sandbars in the nearshore region and therefore onshore sediment transport prevails on the coast. The annual net transport rate towards the southern direction implies that the sediment transition between the berm and nearshore is high during the NE monsoon.

5 Discussion

The present results disclose that the NE and SW monsoons are the predominant cause of beach and nearshore morphological changes on the Nagapattinam coast (Sanil Kumar et al., 2002; Joevivek and Chandrasekar, 2014). The retreating monsoon gusts from the northeast direction having significant moisture bring heavy rainfall along the central Tamil Nadu coast. Frequent tropical cyclones are noticed in this season due to the deep depression formed in the Inter Tropical convergence zone (ITCZ). During the study period, the Nagapattinam coast was highly affected by the tropical cyclone 'Thane'. The surging of waves produced beach ridges and inland sediment deposits all along the coast. The significant wave energy with strong wind force creates onshore sediment transport as well as sandbars at the surf zone. However, the wave climate in fair weather period influences both the magnitude and characteristics of waves for reworking of the beach system.

Field observation implies that Nagapattinam beach experienced dissipative morphodynamic state during the NE monsoon, reflective morphodynamic state during the SW monsoon, and intermediate morphodynamic state during the fair weather condition (Joevivek and Chandrasekar, 2017). The larger width of surf zone during the NE monsoon and shorter during the SW monsoon attests that the bar-berm sediment transition prevails on the coast. These implications are found to be consistent with the results of the wave period, breaking wave height and the longshore current velocity. During the NE monsoon, undertow currents fetch sediments from the beach to the nearshore region which leads to the formation of multiple sandbars at the surf zone. During this period, beach width

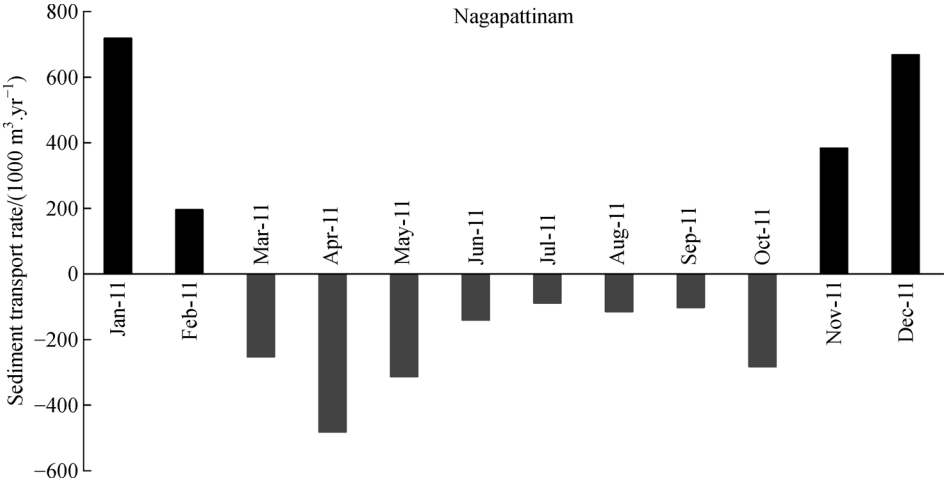

Fig. 7 Longshore sediment transport over an annual cycle (January 2011 to December 2011). Positive direction (black color) represents sediment transport rate during NE monsoon and negative direction (gray color) implies sediment transport rate during SW and fair weather period.

is reduced considerably and the maximum erosion at the foreshore region occurs. Conversely, the beach attained sediment deposition during the SW monsoon. The steep foreshore slope and short surf zone attests that there is either a single bar or no bar is found.

The statistical results provide clear understanding of the relation between beach and wave dynamics. The CCA triplot results show constructive and destructive relationships between beach and nearshore parameters. The positive correlation of the breaking wave height, longshore current velocity, and surf zone width implies that the values of these parameters vary with respect to the nearshore bars. The negative correlations of wave period and beach morphology reveal that the onshore sediment transport prevails in the berm and intertidal region. Similarly, EOF results demarcate the wave response with respect to the beach morphodynamics. The EOF plot clearly depicts propagation of sediments to the nearshore region and vice-versa. Dail et al. (2000) applied EOF technique to examine temporal characteristics of the Waimea Bay, Oahu, Hawaii. They found both the formation and the removal of foreshore dune on the beach and also observed that the sediment migrated from the berm to the foreshore but not the offshore. Larson et al. (2003) investigated Dutch coast and found the formation of new bar near the shoreline as a result of the onshore sediment transport. Jesse (2008) investigated North Carolina beach and found that instability prevailed in the tidal zone due to the strong hurricane and wave action. However, the berm and the backshore clearly depict that there is a seaward movement of sediment during the winter and landward movement during the summer. From these findings and our results, we conclude that monsoonal variation of nearshore process forces rework of sediment distribution in the coastal region.

6 Conclusions

In this paper, a temporal correlation between the beach and wave dynamics is investigated by field observations and empirical models. The field survey revealed that the nearshore process is the primary mechanism for the reworking of sediments in the wave dominated beach system. The beach profile clearly showed the deposition or erosion in the beach system which is controlled by seasonal wave climate. The onshore drive of the divergence wave along with the sediments at full force brings the accumulation of sediments during SW monsoon while the convergence waves enabled maximum erosion during the NE monsoon. The status of the beach morphology and the wave dynamics with respect to the seasonal variation could be clearly understood from EOF results. As observed in the CCA results, the wave period and the beach morphology have positive correlation and the response between them is instantaneous. However, breaking wave height, longshore current velocity, and surf zone width are interlinked and anti-correlated with beach morphology. This implies that there is a sediment transition existing between the beach and the nearshore processes. Moreover, the results from the grain size analysis and sediment transport rate proves that a sediment transition is taking place between the berm and the nearshore region. Overall, Nagapattinam beach experienced short-term erosion during the NE monsoon and long-term recovery during the SW monsoon and the fair weather condition. We confirm that the reworking of sediment transition stabilizes the equilibrium beach condition. The present results will lead a path for the engineering and the marine science community to understand the existence of the sediment transition in the wave dominated beach system.

Acknowledgements The first author is thankful to Mr. P. Vincent Jayaraj, Mr. George Udayaraj, Mr. Duraisamy and Mr. Pushparaj for their effective support during the field survey and Mrs. A. Xavier Leema rose, Mrs. F. Suganya Jenifer, and Ms. K. Shree Purnima for their help in developing the manuscript.

References

Araya-Vergara J F (1986). Toward a classification of beach profiles. J Coast Res, 2(2): 159–165

Bascom W N (1951). The relationship between sand size and beach-face slope. Trans Am Geophys Union, 32(6): 866

Bascom W N (1953). Characteristics of natural beaches. In: Proc 4th Conf Coast Eng, 163–180

Bascom W N (1964). Waves and Beaches: The Dynamics of the Ocean Surface. Garden City N.Y.: Doubleday and Company

Blossier B, Bryan K R, Daly C J, Winter C (2016). Nearshore sandbar rotation at single-barred embayed beaches. J Geophys Res: Ocean, 121(4): 2286–2313

Blott S J, Pye K (2001). GRADISTAT : a grain size distribution and statistics package for the analysis of unconsolidated sediments. Earth Surf Process Landf, 26(11): 1237–1248

Broekema Y B, Giardino A, van der Werf J J, van Rooijen A A, Vousdoukas M I, van Prooijen B C (2016). Observations and modelling of nearshore sediment sorting processes along a barred beach profile. Coast Eng, 118: 50–62

Clark D (1975). Understanding canonical correlation analysis. In: Concepts and techniques in modern geography- No.3. Geo Abstracts Ltd, p 36

Dail H J, Merrifield M A, Bevis M (2000). Steep beach morphology changes due to energetic wave forcing. Mar Geol, 162(2–4): 443–458

Folk R L, Ward W C (1957). Brazos River bar, a study in the significance of grain size parameters. J Sediment Res, 27(1): 3–26

Galvin C J Jr (1968). Breaker type classification on three laboratory beaches. J Geophys Res, 73(12): 3651–3659

Hardoon D R, Szedmak S, Shawe-Taylor J (2004). Canonical correlation analysis: an overview with application to learning methods. Neural Comput, 16(12): 2639–2664

Harley M D, Turner I L, Short A D (2015). New insights into embayed

beach rotation: the importance of wave exposure and cross-shore processes. J Geophys Res: Earth Surf, 120(8): 1470–1484

Horrillo-Caraballo J M, Reeve D E (2011). Application of a statistical method to investigate patterns of beach evolution in the vicinity of a seawall. J Coast Res, SI64: 95–99

Hsu T J, Elgar S, Guza R T (2006). Wave-induced sediment transport and onshore sandbar migration. Coast Eng, 53(10): 817–824

Hunter E R, Edward C, Lawrence P R (1979). Depositional processes, sedimentary structures, and predicted vertical sequences in barred nearshore systems, southern oregon coast. J Sediment Petrol, 49(3): 711–726

Jayakumar S, Raju N S NGowthaman R (2004). Beach dynamics of an open coast on the west coast of India. In: 3rd Indian national conference on Harbour & Ocean engineering, NIO, Goa. 9–16

Jesse H B (2008). Variability in Beach Topography and Forcing Along Oak Island, North Carolina. Dissertation for Master Degree. University of North Carolina Wilmington

Joevivek V, Chandrasekar N (2014). Seasonal impact on beach morphology and the status of heavy mineral deposition – central Tamil Nadu coast, India. J Earth Syst Sci, 123(1): 135–149

Joevivek V, Chandrasekar N (2016). ONWET : a simple integrated tool for beach morphology and wave dynamics analysis. Mar Georesour Geotechnol, 34(6): 581–593

Joevivek V, Chandrasekar N (2017). Data on nearshore wave process and surficial beach deposits, central Tamil Nadu coast, India. Data Brief, 13: 306–311

Larson M, Capobianco M, Jansen H, Rozynshi G, Southgate H N, Stive M, Wijnberg K M, Hulscher S (2003). Analysis of field data of coastal morphological evolution over yearly and decadal time scales. Part 1: background and linear techniques. J Coast Res, 19(4): 760–775

Liu J T, Zarillo G A (1989). Distribution of grain sizes across a transgressive shoreface. Mar Geol, 87(2): 121–136

Maanen B V, Ruiter P J, Coco G, Bryan K R, Ruessink B G (2008). Onshore sandbar migration at Tairua Beach (New Zealand): numerical simulations and field measurements. Mar Geol, 253(3–4): 99–106

Marino-Tapia I J, Russell P E, O'Hare T J, Davidson A, Huntley D A (2007 a). Cross-shore sediment transport on natural beaches and its relation to sandbar migration patterns: 1. Field observations and derivation of a transport parameterization. J Geophys Res: Ocean, 112 (3): C03001

Marino-Tapia I J, Russell P E, O'Hare T J, Davidson A, Huntley D A (2007 b). Cross-shore sediment transport on natural beaches and its relation to sandbar migration patterns: 2. Application of the field transport parameterization. J Geophys Res: Ocean, 112(3):C03002

Masselink G, Austin M, Tinker J, O'Hare T, Russel P (2008). Cross-shore sediment transport and morphological response on a macrotidal beach with intertidal bar morphology, Truc Vert, France. Mar Geol, 251(3 – 4): 141–155

Miller H C (1999). Field measurements of longshore sediment transport during storms. Coast Eng, 36(4): 301–321

Miselis J L, McNinch J E (2006). Calculating shoreline erosion potential using nearshore stratigraphy and sediment volume: outer banks, North Carolina. J Geophys Res: Earth Surf, 111(2): 1–15

Nayak G N, Chavadi V C (1988). Studies on sediment size distribution of North Karnataka beaches, West coast of India, using empirical orthogonal function analysis. Indian J Mar Sci, 17: 63–66

Pape L, Kuriyama Y, Ruessink B G (2010 a). Models and scales for cross-shore sandbar migration. J Geophys Res: Earth Surf, 115(3): 1–13

Pape L, Plant N G, Ruessink B G (2010 b). On cross-shore migration and equilibrium states of nearshore sandbars. J Geophys Res: Earth Surf, 115(3): 1–16

Reis A H, Gama C (2010). Sand size versus beachface slope—An explanation based on the Constructal Law. Geomorphology, 114(3): 276–283

Różyński G (2003). Data-driven modeling of multiple longshore bars and their interactions. Coast Eng, 48(3): 151–170

Ruessink B G, Pape L, Turner I L (2009). Daily to interannual cross-shore sandbar migration: observations from a multiple sandbar system. Cont Shelf Res, 29(14): 1663–1677

Sanil Kumar V, Anand N M, Gowthaman R (2002). Variations in nearshore processes along Nagapattinam coast, India. Curr Sci, 82: 1381–1389

Saravanan S, Chandrasekar N, Joevivek V (2013). Temporal and spatial variation in the sediment volume along the beaches between Ovari and Kanyakumari (SE INDIA). Int J Sediment Res, 28(3): 384–395

Shenoi S S C, Murty C S, Veerayya M (1987). Monsoon-induced seasonal variability of sheltered versus exposed beaches along the west coast of India. Mar Geol, 76: 117–130

Xie S L, Liu T F (1987). Long-term variation of longshore sediment transport. Coast Eng, 11(2): 131–140

Short A D (2012). Coastal Processes and Beaches. Nat Educ Knowl, 3 (10): 15

Splinter K D, Turner I L, Davidson M A, Barnard P, Castelle B, Oltman-Shay J (2014). A generalized equilibrium model for predicting daily to interannual shoreline response. J Geophys Res: Earth Surf, 119(9): 1936–1958

Svensson C (1999). Empirical orthogonal function analysis of daily rainfall in the upper reaches of the Huai River Basin, China. Theor Appl Climatol, 62(3): 147–161

Walton T L, Bruno R O (1989). Longshore transport at a detached breakwater, Phase II. J Coast Res, 5(4): 679–691

Wang P, Kraus N C, Davis R A (1998). Total longshore sediment transport rate in the surf zone: field measurements and empirical predictions. J Coast Res, 14(1): 269–282

Winant C D, Inman D L, Nordstrom C E (1975). Description of seasonal beach changes using empirical eigenfunctions. J Geophys Res, 80 (15): 1979–1986

Wright L D, Short A D (1984). Morphodynamic variability of surf zones and beaches: a synthesis. Mar Geol, 56(1–4): 93–118